Design and analysis of flexible colorless remote node using RSOA-assisted Michelson interferometer

Lei Liu (刘 磊)*, Min Zhang (张 民), Mingtao Liu (刘明涛), Xiaopin Zhang (张小频), and Peida Ye (叶培大)

Key Laboratory of Information Photonics and Optical Communications, Ministry of Education, Beijing University of Posts and Telecommunications, Beijing 100876, China

**Corresponding author: liulei098332@gmail.com*

Received June 12, 2010; accepted November 6, 2010; posted online January 28, 2011

A scheme of flexible colorless remote note with reflective semiconductor optical amplifier (RSOA) assisted Michelson interferometer is proposed. This is capable of generating an optical carrier suppressed signal at a specific radio frequency to suppress the penalty brought about by Rayleigh backscattering and reflection in a full-duplex single fiber transmission network. Simulations are conducted, and the validation of the proposal is discussed by observing the penalty eye opening factor. The results are useful for designing cost-effective multi-wavelength passive optical network (PON) or radio-over-fiber (RoF) systems.

OCIS codes: 060.4510, 060.2360.

doi: 10.3788/COL201109.020606.

Deploying colorless remote nodes (RNs) in multi-wavelength passive optical network (PON) has been considered as an effective solution to the problems of cost and complexity reduction[1−3]. In this environment, many schemes have been proposed to develop low-cost, colorless RNs using tunable lasers, spectrum sliced light sources[4], injection locked lasers, such as Fabry-Perot laser diodes (FP-LDs)[5], or remodulation devices, such as reflective semiconductor optical amplifiers (RSOAs), and reflective electronic absorption modulators (REAMs)[6]. With good amplification and modulation characteristics, the RSOA has become a promising candidate as a remote modulator in colorless RNs. With the help of extra electrical equalization and forward error correction (FEC)[7−10], the modulation bandwidth of RSOA can be enlarged to 10 GHz, indicating a promising prospect for large-scale application. However, the reported RSOA-assisted RNs are vulnerable to crosstalk brought about by the Rayleigh backscattering (RB) and reflections in case of full-duplex communication over a single fiber sharing a single wavelength[11−13]. Some schemes have been proposed, such as frequency-shift keying (FSK) modulation[14] or optical carrier suppressed (OCS) modulation[14−16] with Mach-Zehnder modulator (MZM) in the transmission link, in order to create a frequency shift between the upstream and downstream signals suppressing the crosstalk.

In this letter, a flexible and cost-effective RN with RSOA-assisted Michelson interferometer (RSOA-MI) is presented to generate an OCS signal at radio frequency (RF) located in the upstream that can suppress the crosstalk introduced by RB and reflection by producing a frequency shift between the upstream and downstream.

A schematic diagram of the proposed colorless RN using RSOA-MI is given in Fig. 1, where two RSOAs are located at the ends of the two arms in MI, with one of the arm embedded an optical phase shifter. A group of electronic components, such as local oscillator, mixers, and phase shifters, were applied to generate the upstream RF signals. In the downstream direction, the baseband optical signal was split equally into two parts; these entered the upper and lower arms of RSOA-MI, respectively. These two parts of the signal serving as the seeding light in the RSOAs were remodulated by the upstream electronic RF signals and then reflected afterwards. When the reflected signals re-coupled together, a phase shift was added at the lower arm using an optical delay line. By adjusting the electrical phase shifter and optical delay line, destructive or constructive interference may occur at the coupler with an appropriate phase difference between the two parts of the signals, after which the optical single-sideband (OSSB) or OCS signal emerges at the fiber end from the RSOA-MI. In the OSSB case, the spectrum overlap between the upstream and downstream exists; thus, the penalty introduced by the RB and reflection is still residual. As the simulation results show, about 5-dB-high power is needed to obtain the same performance as in the case of the OCS.

Given that the modulation in RSOA is the result of the interactive process of the photon carrier, the carrier density in the device can be described as[17−19]

$$\frac{\mathrm{d}N(z,t)}{\mathrm{d}t} = \frac{J_{\mathrm{input}}}{q} - \frac{N(z,t)}{\tau_{\mathrm{s}}} - v_{\mathrm{g}} g S, \qquad (1)$$

where the carrier density N is a function of time t and position z along the active layer. The first term on the right is the carrier injection rate, where J_{input} is the injection current density indicating the modulation signal, and q equals the electron charge. The second term is due to spontaneous recombination characterized by the spontaneous carrier lifetime τ_{s}. The third term represents the stimulated recombination leading to optical amplification, v_{g} is the group velocity of the optical signal, g is the gain coefficient, and S is the photon density in the RSOA.

In Eq. (1), the spontaneous carrier lifetime and the

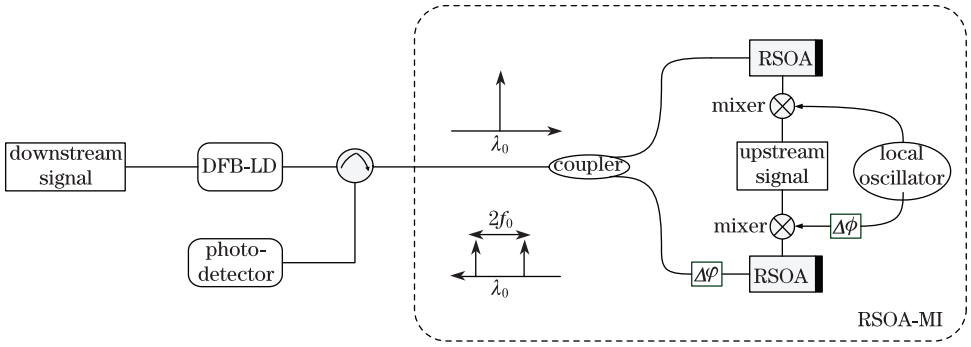

Fig. 1. Schematic diagram of RSOA-MI.

gain coefficient are given by[17]

$$\tau_s = 1/[A + BN(z,t) + CN^2(z,t)], \quad (2)$$

$$g = \frac{a(N - N_0)}{1 + \varepsilon_{NL} S}, \quad (3)$$

where A is the nonradioactive recombination coefficient, B is the coefficient of the spontaneous radioactive recombination, C is the Auger recombination coefficient, a is the differential gain coefficient, N_0 is the transparent carrier density, and ε_{NL} is the nonlinear gain parameter.

The wave propagation in the upper and the lower RSOAs derived from Maxwell's equation is written as[17,19]

$$\pm \frac{\partial E_i(z,t)}{\partial z} + \frac{1}{\nu_g}\frac{\partial E_i(z,t)}{\partial t} = \frac{1}{2}(\Gamma g - \alpha_{int})E_i(z,t) + \mathrm{j}\Gamma k_0 \Delta n_i E_i(z,t), \quad (4)$$

where $E_i(z,\ t)$ is the electric field of the optical signal in the RSOA fixed at the upper or lower of the RSOA-MI, Γ is the optical confinement factor, k_0 is the wave number, Δn_i is the refractive index change induced by current signal injection, α_{int} is the loss coefficient of the active layer, and $\pm$ corresponds to forward and backward propagating waves.

Considering that the ratio of the coupler in Fig. 1 is 50/50, the signal power forming the constructive and destructive ports of the proposed RSOA-MI are given

$$P_{out}(t) = \alpha\{P_{up}(t) + P_{low}(t) \pm 2\sqrt{P_{up}(t)P_{low}(t)}\cos[\Delta\phi_{up}(t) - \Delta\phi_{low}(t)]\}, \quad (5)$$

where $P_{up}(t)$ and $P_{low}(t)$ are the signal power from the upper and lower arms of RSOA, respectively; $\Delta\phi_{up}(t)$ and $\Delta\phi_{low}(t)$ are the phase-shift experienced by RSOA and introduced by the phase shifter, respectively; α is the insertion loss of the coupler. Given that the light wave propagation cannot be solved in analytic expression, the concept can only be proven in subsequent numerical simulations. In order to evaluate our proposed colorless RN, simulations with VPI Transmission Maker 8.3 have been conducted. Figure 2 depicts the simulation diagram of the full duplex communication system with a central office (CO) and a RN detailing the received RF signal spectra and eye diagrams.

In the CO, a 2.5-Gb/s baseband signal generated by a $2^7 - 1$ pseudorandom binary sequence (PRBS) is directly driving the distributed feedback laser diode (DFB-LD), acting as the optical carrier of both upstream and downstream signals. In order to maintain the polarization statement of the downstream signal, a polarization controller (PC) was fixed after the DFB-LD. After the transmission along the 40-km single mode fiber with a RB coefficient of 5×10^{-5} km^{-1}, the downstream signal was injected into the RN and then divided into two parts with a ratio of 2:8 at the coupler to excite the RSOA with a high power serving as the upstream carrier, while the part with low power was detected by the photodetector as the downstream signal.

At the RN, a 1.25-Gb/s PRBS data was equally divided and mixed with the RF signal to emerge the optical RF signal at the RSOA-MI. A wide-band RF generator was used to generate an adjustable RF signal. According

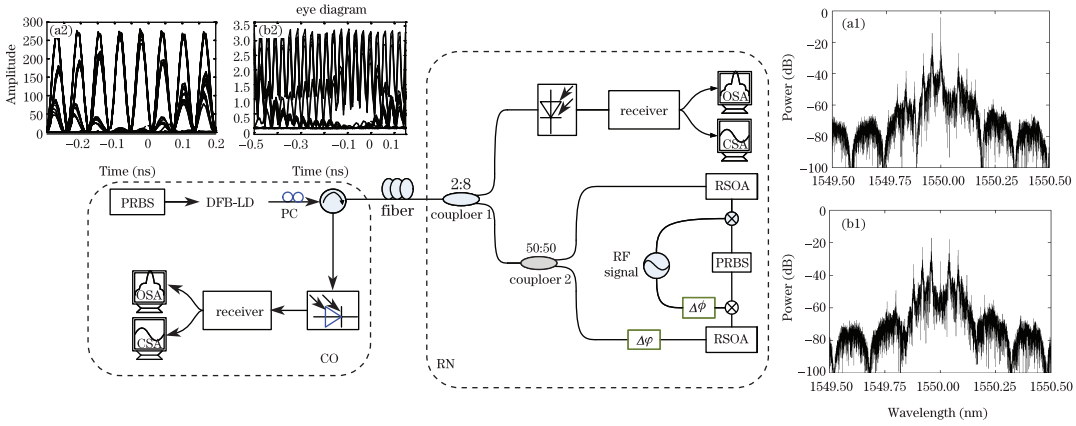

Fig. 2. Simulation arrangement for the proposed remodulation system with RSOA-MI.

to the principle described above, by adjusting the optical and the electrical phase shifters at the two arms of MI ($\Delta\Psi$ and $\Delta\Phi$), the OSSB or OCS signal can be achieved in the upstream.

The output optical spectra of RSOA-MI are the direct validations of this proposal. The optical spectra from "coupler2" are presented in Figs. 2(a1) and (b1). Equation (3) shows that a dedicated modulation format is achieved by adjusting the phase shifters $\Delta\Phi$ and $\Delta\Psi$. If $\Delta\Phi = \pi/2$ and $\Delta\Psi = 0$ (Fig. 2 (a1)), and that only a single sideband is reserved. Similarly, by altering the phase shifter as: $\Delta\phi = \pi$ and $\Delta\varphi = \pi/4$ (in the bidirectional transmission, the optical phase shift should be set as half of that in the unidirectional one), the optical carrier is suppressed. The received RF signal eye diagrams launched from the RSOA-MI are given in Figs. 2(a2) and (b2), for the OSSB and OCS scenarios, respectively. Moreover, as the simulation indicates, the phase delay need not be precisely equal to the value set before, and a slight difference less than 10° is tolerant.

The curves of the penalty eye opening factor (EOF) versus the received power are given to indicate the transmission quality of the system (Fig. 3). In this simulation, we used EOF as gauge (EOF = 1 equals bit error rate (BER)=10^{-9}), and a variable attenuator was installed before the receiver to obtain the appropriate receiving power. Obviously, under the same transmission conditions, the OCS signals demonstrated better performance. In the OCS scenario, both the upstream and downstream signals suffered little degeneration caused by the introduction of the optical fiber with a relatively low bit rate. In the OSSB scenario, due to the interaction between the main peaks of the upstream signal and the downstream baseband signal, the degeneration is about 5 dB for both uplink and downlink in comparison with the OCS scenario.

The downstream signal wavelength and the modulation formats are investigated in order to find the optimal configuration for the scheme, the influence on the system performance exerted by the bias current. In the simulations, the parameters used in calculations were set as representative values for commercial InGaAsP semiconductor materials operating at approximately 1550 nm (Table 1).

Figure 4 presents the effect of bias current on the performance of the proposed RSOA-MI with 0.5-mm-long active layer. The downstream transmit powers were set as –20, –15, and –10 dBm, and the frequency of RF signal was at 5 GHz. As the bias current increases, the penalty of EOF reaches an optimum result. At first, the carrier density and the photon density grew with the bias current resulting in good modulation characteristic, but when the bias current exceeded the threshold, the spontaneous emission noise rose greatly and distorted the re-modulated signal. The most suitable bias current for RF signal modulation is ∼55–61 mA (Fig. 4).

The wavelength adaption is a key factor for wavelength-division multiplexing (WDM) PON arrangement, and in this proposal the span of the operational wavelength at the RSOA-MI is analyzed. Simulations proceeded with the wavlength ranging from 1520 to 1620 nm, while the downstream transmitting power was set as −10, −5, and 0 dBm. In the upstream, OCS modulation formats were

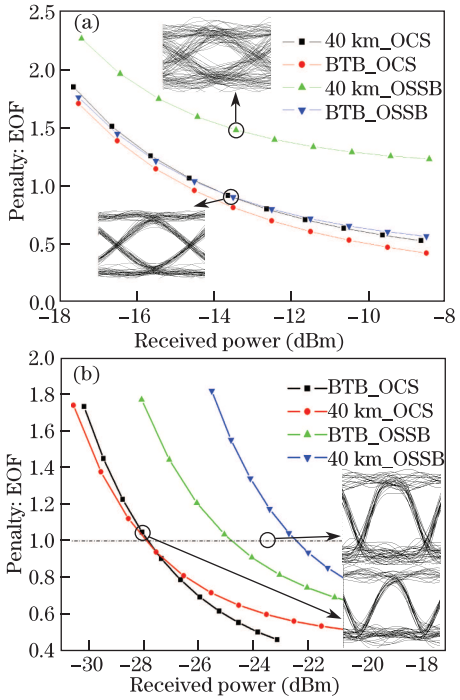

Fig. 3. Penalty EOF curves and eye diagrams of the system. (a) EOF measurements of the 1.25-Gb/s directly modulated baseband downstream signal; (b) EOF measurements of 1.25-Gb/s RF band upstream signal with both OCS and OSSB modulation formats.

Table 1. Parameters List for the RSOA

Physical Parameters	Value	Units
Active Length (L)	0.0003	m
Taper Length (L)	0.0002	m
Width (w)	6×10^{-7}	m
Height (h)	4×10^{7}	m
Active Area (A_{eff})	2.4×10^{-13}	m^2
Optical Confinement Factor (Γ)	0.3	
Gain Constant (a_0)	2.5×10^{-20}	m^2
Carrier Density at Transparency (N_0)	1.4×10^{24}	m^{-3}
Nonlinear Gain Parameter (ε_{NL})	1.2×10^{-22}	m^3
Recombination Coefficient (A)	3.6×10^{8}	1/s
Recombination Coefficient(B)	5.6×10^{-16}	m^3s^{-1}
Auger Recombination Coefficient (C)	3×10^{-41}	m^6s^{-1}

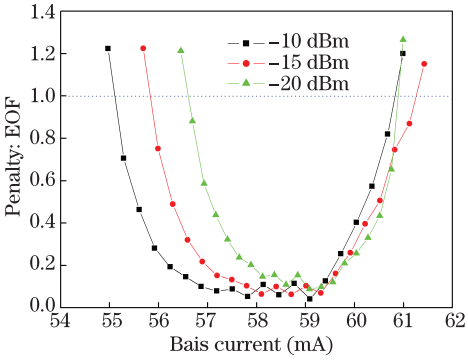

Fig. 4. Penalty of EOF of the upstream signal versus bias current with OCS modulated format signal.

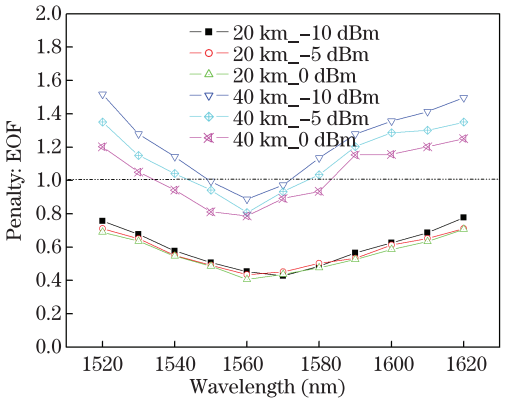

Fig. 5. Penalty of EOF of the upstream signal versus wavelength.

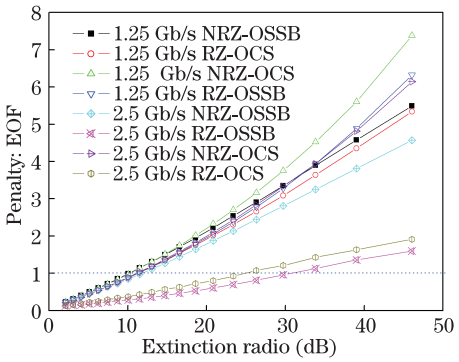

Fig. 6. System performance measurements with different signal formats.

used with a 60-mA bias current. In the network with a coverage of 20 km, the operational wavelength span of the RSOA-MI was set at over 100 nm (Fig. 5), and the the operational wavlength span of the RSOA-MI was reduced to 60 nm when the input power was set at 0 dBm.

Analysis of the influence of the signal formats and the extinction radio (ER) on the performance of the RSOA-MI is also conducted. The increase of the ER resulted in performance degradation (Fig. 6). By working at a linear region, RSOA modulation suffered great impact from the pattern effect. Consequently, the appropriate pulse width and ER should be selected. In this simulation, the ER of the downstream signal should be no larger than 9 dB.

In conclusion, a flexible, colorless remodulation node has been proposed and numerically demonstrated. Based on the proposed RSOA-MI structure, the OCS signal can be generated in the uplink to suppress the crosstalk brought about by the RB and reflection. As the key device of the proposal, the influences of the RSOA parameters on the system performance have also been simulated and analyzed. A list of the pertinent parameters for RF signal remodulation has been given for further research and experimental verification. Thanks to the compact size of RSOA, this scheme can be integrated in next generation multi-wavelength PON or ROF networks.

This work was supported by the National Natural Science Foundation of China (No. 61072008), the "863" Program of China (No. 2009AA01z255), the "111" Project of China (No. B07005), the Beijing New Star Program of Science and Technologies (No. 2007A048), Fundamental Research Funds for Central Universities (Nos. 2009GYBZ and 2009RC0401), and the Program for Excellent Talents in BUPT.

References

1. G. Berrettini, G. Meloni, L. Giorgi, F. Ponzini, F. Cavaliere, P. Ghiggino, L. Poti, and A. Bogoni, Photon. Technol. Lett. **21,** 453 (2009).
2. K. Y. Cho, Y. J. Lee, H. Y. Choi, A. Murakami, A. Agata, Y. Takushima, and Y. C. Chung, J. Lightwave Technol. **27,** 1286 (2009).
3. E. T. Lopez, J. A. Lazaro, C. Arellano, V. Polo, and J. Prat, Photon. Technol. Lett. **22,** 97 (2010).
4. J. Prat, M. Omella, and V. Polo, in *Proceedings of OFC 2007* OTuG6 (2007).
5. H. D. Kim, S.-G. Kang, and C.-H. Le, Photon. Technol. Lett. **12,** 1067 (2000).
6. D. Smith, I. Lealman, X. Chen, D. Moodie, P. Cannard, J. Dosanjh, L. Rivers, C. Ford, R. Cronin, T. Kerr, L. Johnston, R. Waller, R. Firth, A. Borghesani, R. Wyatt, and A. Poustie, in *Proceedings of ECOC 2009* 8.6.3 (2009).
7. K. Y. Cho, Y. Takushima, and Y. C. Chung, Photon. Technol. Lett. **20,** 1533 (2008).
8. B. Schrenk, G. de Valicourt, M. Omella, J. A. Lazaro, R. Brenot, and J. Prat, Photon. Technol. Lett. **22,** 392 (2010).
9. K. Y. Cho, A. Agata, Y. Takushima, and Y. C. Chung, Photon. Technol. Lett. **22,** 57 (2010).
10. E. Zhou, X. Zhang, and D. Huang, Opt. Express **15,** 9096 (2007).
11. J.-M. Kang, Y.-Y. Won, S.-H. Lee, and S.-K. Han, in *Proceedings of OFC 2006* JThB68 (2006).
12. H. Hu and H. Anis, J. Lightwave Technol. **26,** 870 (2008).
13. Y. Takushima, K. Y. Cho, and Y. C. Chung, in *Proceedings of IEEE Photonics Global 2008* (2008).
14. J. Prat, C. Arellano, V. Polo, and J. A. Lazaro, in *Proceedings of ECOC 2006* (2006).
15. C. W. Chow, G. Talli, A. D. Ellis, and P. D. Townsend, Opt. Express **16,** 1860 (2008).
16. T. T. Pham, H.-S. Kim, Y.-Y. Won, and S.-K. Han, in *Proceedings of OFC/NFOEC 2009* OThA2 (2009).
17. N. Cheng and L. G. Kazovsky, Proc. SPIE **6468,** 64680V-1 (2007).
18. M. A. Ali, A. F. Elrefaie, and S. A. Ahmed, Photon. Technol. Lett. **4,** 280 (1992).
19. J.-M. Kang, W. Shim, H. Kwon, T. Kim, and S.-K. Hau, in *Proceedings of OFC 2004* OTuB3 (2004).